Physical Communication 62 (2024) 102255

Contents lists available at ScienceDirect

Physical Communication

journal homepage: www.elsevier.com/locate/phycom

Full length article

BEP evaluation of 5G LDPC codes in a pre-amplified optical PPM receiver

Konstantinos Yiannopoulos *, Nikos C. Sagias

Department of Informatics and Telecommunications, University of Peloponnese, Akadimaikou G.K. Vlahou, Tripoli, 22131, Arcadia, Greece

ARTICLE INFO

Keywords:
Optical amplification
Pulse-position modulation
Low-density parity-check codes

ABSTRACT

We present results for the performance of a pre-amplified optical pulse-position modulation (PPM) receiver that utilizes the low-density parity-check (LDPC) correction codes of the 5G standard. The code construction is suitable for correcting burst errors that are introduced by PPM. Simulation results show that the LDPC codes can provide a very significant real gain, provided that the code rate is chosen appropriately. We find that the code rates that minimize the bit-error-probabilities (BEPs) of the system range between 2/3 and 22/26, with higher code rates being required in receivers that operate under increased optical noise. It is also shown that a comparable real gain is obtained for both the sum–product and min-sum decoders, while the power penalty of the latter one is only limited to 0.2 dB, when the aforementioned code rates are utilized.

1. Introduction

The implementation of reliable and high-capacity optical wireless communication links, calls for highly sensitive optical receivers and a number of technologies have been investigated towards their realization [1–5]. Optical amplification and orthogonal modulations like PPM have been particularly appealing, since they drastically lower the number of received photons that are required for low BEPs. The errors are typically corrected via coding and a number of coding schemes have been previously employed, including Reed–Solomon, convolutional, Turbo and LDPC codes [6–15]. LDPC codes, in particular, have been shown to perform close to the Shannon limit [16–18] and have been recently included as one of the two coding options in the 5G standard [19].

A key feature of the LDPC codes in the 5G standard is that the construction of the parity check matrix relies on permutations of the $Z_c \times Z_c$ identity matrix (blocks). As a result, the parity checks are performed among data bits that are not located within the same block, and short bursts of errors within a block can be efficiently corrected. PPM introduces such types of burst errors, since an erroneous symbol will affect up to $\log_2(Q)$ bits, where Q is the modulation order. The errors will be corrected assuming that $Z_c \gg \log_2(Q)$, which is true for most practical systems, since Z_c is determined by the data length and large lengths are required for a better decoding performance. This approach is compatible with the independent encoding and decoding of the individual bits that construct each PPM symbol, which has been shown to provide an effective method of error correction in optical channels [20]. The LDPC decoders introduce additional message exchanges between the individual single parity check decoders and therefore even better error correction is expected.

The apparent compatibility between PPM and the 5G LDPC codes has been the instigation for this work. The novelty of our analysis relies on modeling the receiver noise with χ^2 distributions [21,22], which have been shown to present an accurate description of the pre-amplified system both theoretically and experimentally [23,24], and have been extensively utilized in the literature [3,15,25,26]. To our knowledge, previous works on error correction via soft-decision decoding of LDPCs have focused on on–off keying [25] and this is the first time that the χ^2 distribution has been considered in the performance evaluation of a PPM receiver. As a result, we have been able to provide novel and accurate results for the real gain of the 5G LDPCs in a pre-amplified optical system. The real gain is defined as the coding gain minus the energy penalty that is introduced due to the increase in the number of transmitted bits.

We show via simulations that the LDPCs can provide a real gain between 2 dB and 4 dB provided that an appropriate code rate is utilized. The identification of the optimal code rates is a key contribution of this work since a high power penalty is observed when the code rates significantly deviate from the optimal value. The code rates that optimize the performance, in the sense that they require the lowest energy to enter the waterfall region, range between 2/3 and 22/26 with the exact value depending mainly on the optical noise modes that enter the receiver. This holds true for both the min-sum and sum–product decoding algorithms [27], while the results also show that the utilization of the optimal code rates reduces the power penalty that has been observed between the two decoders [28]. It is demonstrated that the use of the min-sum decoder introduces a penalty of 0.2 dB or less for a range of data lengths assuming optimal code rates, thus alleviating

* Corresponding author.
E-mail address: kyianno@uop.gr (K. Yiannopoulos).

https://doi.org/10.1016/j.phycom.2023.102255
Received 14 March 2023; Received in revised form 31 October 2023; Accepted 3 December 2023
Available online 6 December 2023

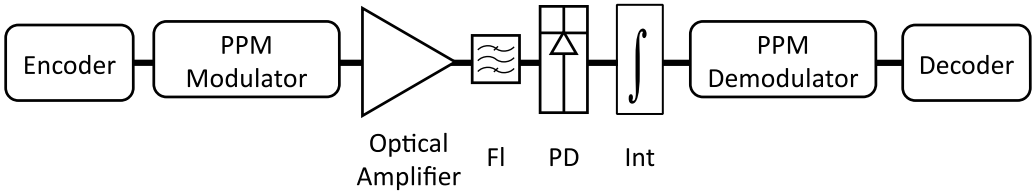

Fig. 1. Setup for the optically pre-amplified PPM communication system. Fl: optical filter, PD: photodiode, Int: integrator.

the need for modifying its operation [28–31]. This is the case for both 4- and 16-PPM systems, as well as systems with narrow- and broad-band optical filters.

The introduction of the χ^2 distributions, however, comes at the expense of complexity, since the calculation of the likelihoods that are required by the decoders requires $Q/\log_2(Q)$ evaluations of a hyper-geometric series per received bit [25]. To mitigate this complexity, we also propose an efficient approximation that completely avoids the hyper-geometric series and relies on identifying the maximum signals on predetermined positions of the PPM symbol, which is a significantly simpler task to perform. The approximation is highly accurate for systems with large optical bandwidths, which are considered for real-world realizations, and introduces a deviation of less than 0.1 dB.

The rest of this paper is structured as follows: Section 2 discusses the LDPC code construction, as well as the sum–product and min-sum decoding algorithms. The χ^2 reception model is described in detail, along with the calculation of the extrinsic information that is required by both decoders. The simulation results for both decoders are presented in Section 3, where it is also shown that they exhibit comparable BEP performance. Section 4 details the proposed approximation for the calculation of the extrinsic information, and presents simulation results that validate its accuracy. Finally, Section 5 summarizes the findings and concludes the paper.

2. System models

The setup under consideration is shown in Fig. 1. The data are encoded using LDPC codes and the resulting codeword is partitioned in PPM symbols. At the receiving side, the signal is amplified, while corrupted by optical noise from the amplifier. The signal is filtered in the optical domain and the noisy symbols are detected on a photodiode. The electrical current is integrated over each PPM slot duration, and the resulting signal values are utilized by the demodulator to estimate the transmitted PPM symbol and the corresponding bits. The received bits are grouped into codewords that are processed by the decoder to reconstruct the original data stream. The encoder/decoder, receiver and modulator/demodulator operations are presented in more detail in the following subsections.

2.1. LDPC encoder and decoder

The quasi-cyclic parity-check matrix structure of the 5G standard is used to generate the codewords [19]. In this approach, the base parity-check matrix consists of smaller block matrices of size $Z_c \times Z_c$ and an appropriate number of block rows and columns. The matrices are either zero matrices or cyclic permutations of the identity matrix and their positions on the block rows and columns are determined using the set index i_{LS}, which contains Z_c. For the Base Graph 1 (BG1), which is oriented towards larger data lengths up to 8448 bits, the maximum number of block columns and rows equals 68 and 46, respectively. The first $K_b = 22$ columns are always assigned to the data. In a similar fashion, BG2 supports smaller data lengths up to 3840 bits, and therefore is limited to 52 block columns and 42 block rows. The first $K_b = 10$ block columns correspond to the data. In this work we only consider data lengths equal to $K = Z_c \times K_b$, thus, we fully utilize the available data columns and avoid padding and/or puncturing. The parity-check matrix for the desired code rate R_c is attained by selecting first K_b/R_c block columns and $K_b(1-R_c)/R_c$ block rows of the corresponding base matrix. The data lengths and rates that have been investigated in this work are summarized in Table 1, along with the associated K_b, Z_c and i_{LS} values.

Table 1
LDPC code parameters.

K (bits)	Code rate	BG	K_b	Z_c	i_{LS}
1280	1/2, 2/3	2	10	128	0
1320	22/26	1	22	60	7
8448	1/3, 1/2, 2/3, 22/26	1	22	384	1

The encoder utilizes the double-diagonal structure of the parity block columns $(K_b+1, K_b+2, \ldots, K_b/R_c)$ to efficiently calculate the parity bits and construct the codeword. In contrast with the 5G standard, the codeword is not shortened or punctured and all $N = K/R_c$ bits are transmitted to the decoder. Two decoders were implemented based on the sum–product and min-sum iterative message passing algorithms [32, eq. (22)]. Both algorithms utilize messages $\alpha_{m,n}$ (variable-to-check) and $\beta_{m,n}$ (check-to-variable) to calculate the intrinsic LLR γ_n [31]. The sum–product decoder updates messages $\beta_{m,n}$ following

$$\beta_{m,n} = 2\tanh^{-1}\left[\prod_{n'\in P_m\setminus\{n\}} \tanh\left(\frac{\alpha_{m,n'}}{2}\right)\right], \tag{1}$$

while the min-sum utilizes the approximation

$$\beta_{m,n} = \prod_{n'\in P_m\setminus\{n\}} \operatorname{sgn}\left(\alpha_{m,n'}\right) \min_{n'\in P_m\setminus\{n\}} |\alpha_{m,n'}|, \tag{2}$$

where $P_m \setminus \{n\}$ denotes the positions of the non-zero entries of the parity-check matrix at row m, except for column n itself. The intrinsic LLR and the new values for $\alpha_{m,n}$ are calculated from

$$\alpha_{m,n} = \gamma_n - \beta_{m,n}, \tag{3}$$

with

$$\gamma_n = \rho(b_n) + \sum_{m\in P_n} \beta_{m,n}, \tag{4}$$

where P_n denotes the positions of the non-zero entries of the parity-check matrix at column n and $\rho(b_n)$ is the extrinsic LLR of the nth bit and its calculation is presented in the next section. The message update process is iterated until a valid codeword is found, or when a maximum number of iterations has been performed. In our implementation, the maximum number of iterations is limited to 10 for both decoders.

2.2. Receiver and PPM demodulator

The optical signal is modulated using PPM and each PPM symbol comprises Q successive time-slots. One of the slots carries the symbol

energy and all other $Q-1$ slots are empty. In the receiving side, we consider an IM/DD receiver, where the incoming optical signal is optically amplified and filtered prior to square law detection. At the output of the amplifier, the energy-containing slot is magnified by the amplifier gain G, while all Q slots are corrupted by the amplifier noise. The optical signal is converted to electrical, with the help of a square law detector, and the output signal is integrated over the duration of the Q slots, to generate the signal vector $\mathbf{s} = (s_1, s_2, \ldots, s_Q)$ for each received symbol. The $\mathbf{s}$ vector components correspond to central $\chi^2_{k,0}$ random variables (RV)s in the $Q-1$ slots, that do not have any signal energy, and a non-central $\chi^2_{k,\lambda}$ RV in the slot that has the signal energy, with k denoting the noise modes. The corresponding probability density functions (pdf)s are [22]

$$p_e(x;k) = \frac{x^{k-1}}{(k-1)!}\,\exp(-x) \tag{5}$$

and

$$p_s(x;k,\lambda) = \exp[-(x+\lambda)]\left(\frac{x}{\lambda}\right)^{\frac{k-1}{2}} I_{k-1}\left(2\sqrt{\lambda\, x}\right), \tag{6}$$

where $I_n(\cdot)$ denotes the modified Bessel function of the first kind. In the previous equations λ is the symbol energy to noise ratio

$$\lambda = \frac{K}{N}\frac{E}{N_0} = \frac{K}{N}\frac{E_b}{N_0}\log_2(Q), \tag{7}$$

where E_b is the energy per bit after amplification, $N_0 = n_{sp}\, h\, f\, (G-1)$ is the optical noise spectral density, n_{sp} is the spontaneous emission factor of the amplifier and $h\, f$ is the photon energy.

The LDPC decoder requires an extrinsic LLR to be associated with each received bit b_ℓ within the PPM symbol following

$$\rho(b_\ell) = \log\left[\frac{P(b_\ell = 0|\mathbf{s})}{P(b_\ell = 1|\mathbf{s})}\right]. \tag{8}$$

We note that the ℓ-th bit is '0' for $Q/2$ of the PPM symbols and '1' for the rest and define the resulting slot sets as B^0_ℓ and B^1_ℓ, since the sets are different for the each of the $\ell = 1, 2, \ldots, \log_2(Q)$ bits in the PPM symbol [33]. For example, in 4-PPM the four slots represent the bit combinations $\{00, 01, 10, 11\}$ and the sets equal $B^0_1 = \{slot\ 1, slot\ 2\}$, $B^1_1 = \{slot\ 3, slot\ 4\}$ for the first bit, and $B^0_2 = \{slot\ 1, slot\ 3\}$, $B^1_2 = \{slot\ 2, slot\ 4\}$ for the second. The probability that a bit is '0' or '1' is calculated from the sum of the symbol probabilities in each corresponding set and the LLR becomes

$$\begin{aligned}\rho(b_\ell) &= \log\left[\frac{P(b_\ell = 0|\,\mathbf{s})}{P(b_\ell = 1|\mathbf{s})}\right] = \log\left[\frac{P\left(\bigcup_{i\in B^0_\ell} s_i\middle|\mathbf{s}\right)}{P\left(\bigcup_{i\in B^1_\ell} s_i\middle|\mathbf{s}\right)}\right] \\ &= \log\left[\frac{\sum_{i\in B^0_\ell} P(s_i|\mathbf{s})}{\sum_{i\in B^1_\ell} P(s_i|\mathbf{s})}\right].\end{aligned} \tag{9}$$

Assuming that the PPM symbols occur with equal probabilities, the appearing a-priori probabilities are given by [7, eq. (10)]

$$P(s_i|\mathbf{s}) = \frac{\Lambda\left(s_i;k,\lambda\right)}{\sum_{n=1}^{Q}\Lambda\left(s_n;k,\lambda\right)}, \tag{10}$$

where $\Lambda(\cdot)$ is the likelihood function. Assuming also χ^2 statistics in the $\mathbf{s}$ vector components, the likelihood function is calculated from

$$\begin{aligned}\Lambda\left(s_i;k,\lambda\right) &= \frac{p_s\left(s_i;k,\lambda\right)}{p_e\left(s_i;k\right)} = \exp(-\lambda)\,(k-1)!\,\frac{I_{k-1}\left(2\sqrt{\lambda\, s_i}\right)}{\left(\sqrt{\lambda\, s_i}\right)^{k-1}} \\ &= \exp(-\lambda)\,{}_0F_1\left(;k;\lambda\, s_i\right),\end{aligned} \tag{11}$$

with ${}_pF_q(\cdot;\cdot;\cdot)$ denoting the generalized hypergeometric function [34, eq. (9. 14.1/MO 1)]. Using (10) and (11), the extrinsic LLR of each bit is calculated from

$$\rho(b_\ell) = \log\left[\frac{\sum_{i\in B^0_\ell}{}_0F_1(;k;\lambda\, s_i)}{\sum_{i\in B^1_\ell}{}_0F_1(;k;\lambda\, s_i)}\right]. \tag{12}$$

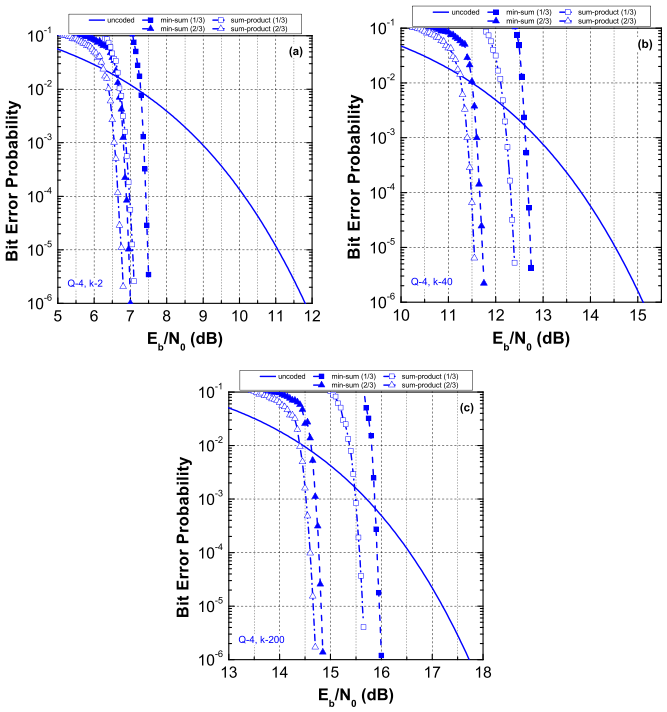

Fig. 2. BEP for the LDPC coded 4-PPM receiver. The data length is $K = 8448$ bits.

3. Results and discussion

The performance of the system was evaluated using Monte-Carlo (MC) simulations. To this end, random data bits were coded using the corresponding encoder and were then converted to PPM symbols. The empty slots were mapped to randomly generated $\chi^2_{k,0}$ variables and the energy slots were mapped to randomly generated $\chi^2_{k,\lambda}$ variables. The PPM demodulator utilized (12) to calculate the extrinsic LLRs for the LDPC decoder. The decoder output was compared with the original data bits and the BEP was estimated by counting the errors over multiple successive decodings. The simulations were performed for a confidence level of 99% and the confidence interval upper and lower limits were calculated following [35, eq. (11.2.11)]. The simulation persisted until the width of the confidence interval, relative to the measured BEP value, was less than 10%, which ensured that the upper and lower endpoints of the interval practically coincided with the BEP estimation.

Figs. 2 and 3 present results for 4- and 16-PPM and $k = 2$, 40, 200 noise modes. The data length is fixed to the maximum length of the 5G standard ($K = 8448$ bits), which is expected to achieve the best BEP performance, while the code rate is set to 1/3 and 2/3. The uncoded system BEP is obtained using [26, eq. (15)] and is included for comparison purposes. The results show that a high real gain is attained for all modulation order and noise mode scenarios. The gain is dependent on both parameters, and lower gains are observed as either the modulation order or the noise modes increase. Assuming a target BEP of 10^{-5} and a code rate of 1/3, the highest gain is equal to 4.0 dB and is observed for $Q = 4$, $k = 2$, while the lowest is equal to 0.5 dB for $Q = 16$, $k = 200$. A code rate of 2/3 achieves a better performance and provides an additional gain of 0.5 dB for $Q = 4$, $k = 2$, which further improves as the modulation order and noise modes increase and attains a value of approximately 1.5 dB for $Q = 16$, $k = 200$.

The preceding discussion suggests that higher code rates are more efficient, especially when the modulation order and/or noise modes increase. To further explore this result and identify the best possible code rate selection, we simulated the system for code rates up to 22/26, which is the maximum in the 5G standard, and the results are shown

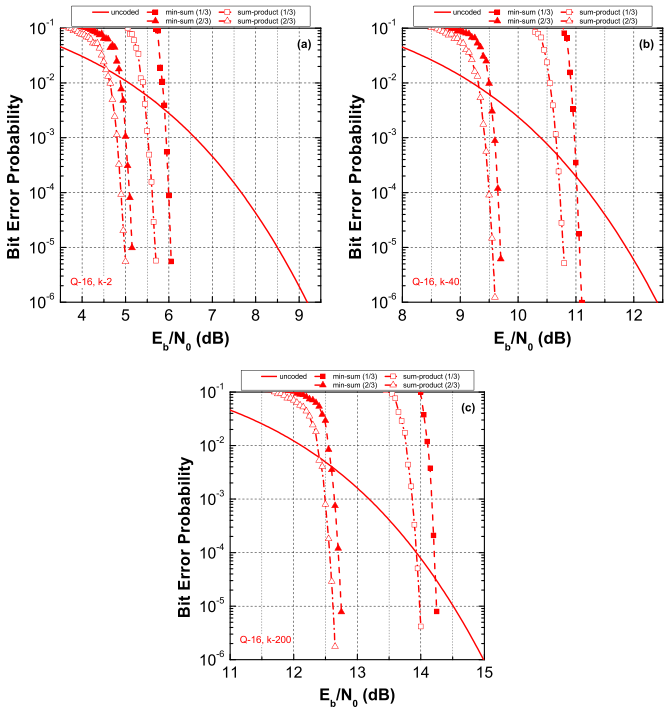

Fig. 3. BEP for the LDPC coded 16-PPM receiver. The data length is $K = 8448$ bits.

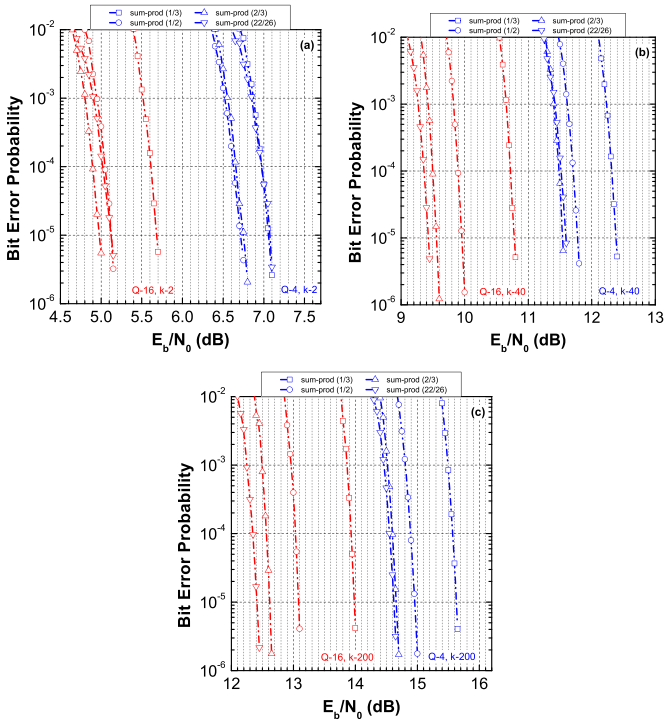

Fig. 4. BEP dependence of the sum–product decoder on the code rate. The data length is $K = 8448$ bits.

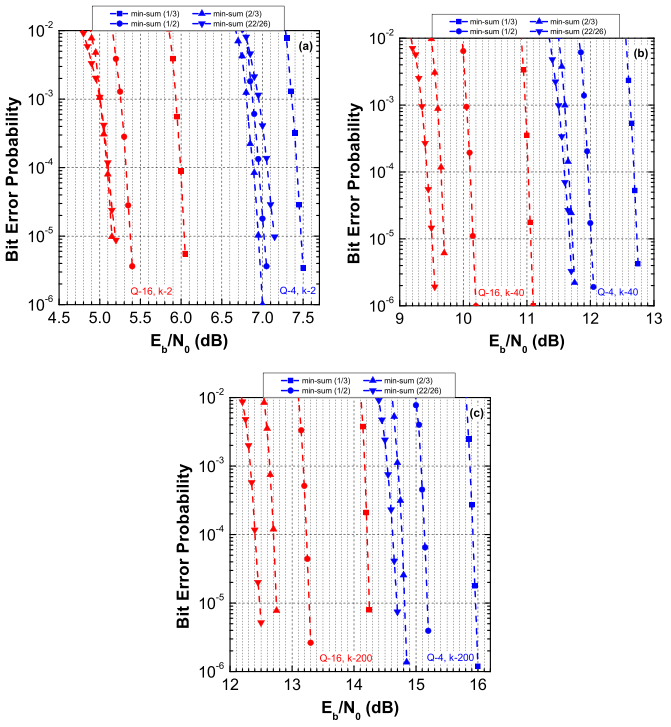

Fig. 5. BEP dependence of the min-sum decoder on the code rate. The data length is $K = 8448$ bits.

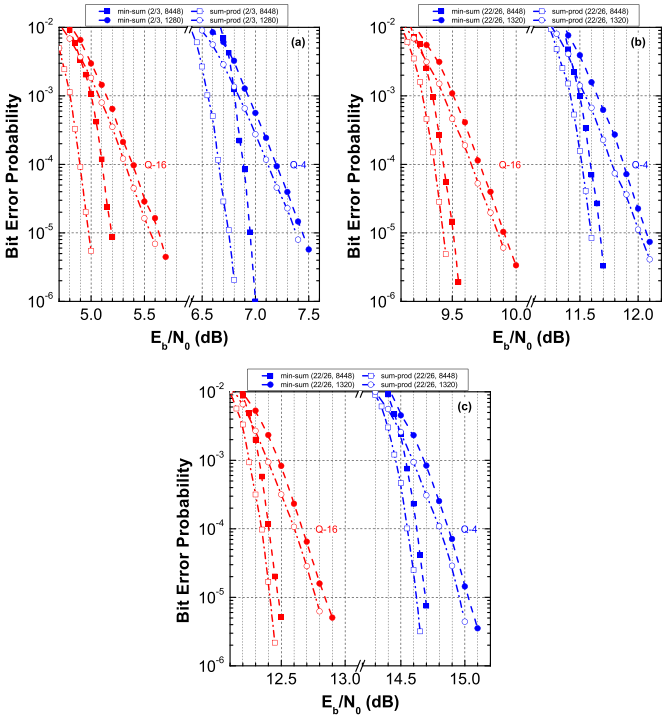

Fig. 6. Comparison of the sum–product and min-sum decoders when optimal code rates are considered. The noise modes are equal to (a) $k = 2$, (b) $k = 40$ and (c) $k = 200$.

in Figs. 4 and 5. For $k = 2$ noise modes the optimal rate is 2/3, except for 4-PPM with the sum–product decoder where a 1/2 rate provides a limited gain of less than 0.1 dB. Similarly, the optimal rate is 22/26 for $k = 40$ noise modes, again with the exception of the 4-PPM sum–product decoder that requires a code rate 2/3 to attain an equally limited gain. Finally, the optimal code rate for $k = 200$ noise modes equals 22/26 for both types of decoders and modulation orders. As a result, the selection of the optimal code depends primarily on the noise modes that enter the receiver and evidently the code rate increases with the noise modes.

The simulation results also show that the sum–product decoder performance is superior to the min-sum one. However, the two decoders

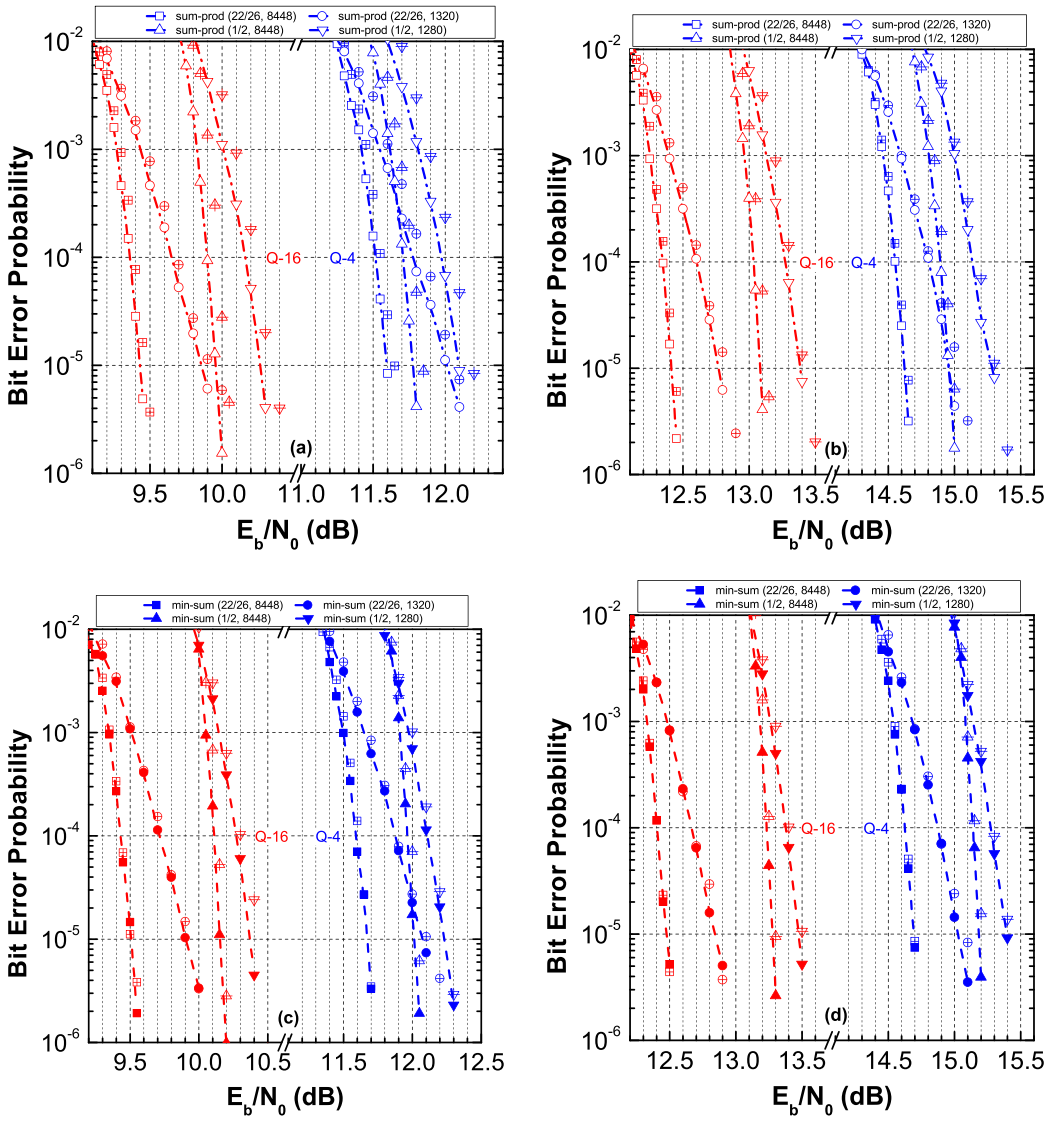

Fig. 7. Decoder performance for the exact and approximated extrinsic LLR. (a) and (b) correspond to the sum–product decoder with $k = 40$ and $k = 200$, respectively. (c) and (d) correspond to the min-sum decoder $k = 40$ and $k = 200$, respectively. The symbols with crosses present the approximate results.

perform closely in systems that utilize the aforementioned code rates that achieve the minimum BEP. The comparison of the two decoders is detailed in Fig. 6, where it can be verified that the penalty that is introduced from the use of the min-sum decoder is equal to 0.2 dB for $k = 2$ noise modes and reduces when the noise modes increase. This is also the case for smaller data lengths equal to $K = 1280$ and $K = 1320$ bits for a rate of 2/3 and 22/26, respectively, as well as intermediate lengths. The min-sum decoder is therefore particularly appealing, given that it is relatively accurate, easier to implement and it also allows for a significant simplification of the extrinsic LLR calculation as we demonstrate in the next section.

4. Approximation of the extrinsic LLR

The exact evaluation of the extrinsic LLR, with the help of (12), requires the calculation of the likelihood for the signals that have been received in all slots. This proves to be time consuming due to the dependence of the LLR on the hyper-geometric function, especially as the modulation order, noise modes and E_b/N_0 increase. With the goal to simplify the evaluation of the LLR, we approximate the sums inside the logarithm with the maximum term, assuming that the rest of the terms do not contribute significantly [36, eq. (8)]

$$\rho(b_\ell) \approx \log\left[\frac{\max_{i\in B_\ell^0} {}_0F_1(;k;\lambda s_i)}{\max_{i\in B_\ell^1} {}_0F_1(;k;\lambda s_i)}\right]. \tag{13}$$

This approximation is usually used to reduce the computational complexity and can be justified from the increasing behavior of the hyper-geometric function. However, it still requires the evaluation of the hyper-geometric function in the slots that were identified by the max operation, thus partially maintaining the computational overhead. To fully eliminate the evaluation of the hyper-geometric function, we propose a second approximation that replaces the χ^2 pdfs with gaussians following

$$\begin{aligned} p_e(x;k) &\approx \frac{1}{\sqrt{2\pi k}} \exp\left[-\frac{(x-k)^2}{2k}\right] \\ p_s(x;k,\lambda) &\approx \frac{1}{\sqrt{2\pi(k+2\lambda)}} \exp\left[-\frac{(x-k-\lambda)^2}{2(k+2\lambda)}\right], \end{aligned} \tag{14}$$

where we have utilized the first and second order moments of the χ^2 distributions to match the corresponding moments of the gaussian distributions. This leads to a gaussian approximation of the hyper-geometric function as well, and, after some algebraic manipulations,

(13) simplifies to

$$\rho(b_{\ell}) \approx \frac{\lambda}{k\,(k+2\,\lambda)} \left(\max_{i \in B_{\ell}^{0}} s_i - \max_{i \in B_{\ell}^{1}} s_i \right) \left(\max_{i \in B_{\ell}^{0}} s_i + \max_{i \in B_{\ell}^{1}} s_i - k \right). \tag{15}$$

Eq. (15) provides a particularly simple calculation method for the LLR since it only requires the maximum values of the signals that have been received in the PPM slots. Moreover, it can be further simplified for the min-sum decoder, where it is possible to omit the constant $\lambda/(k\,(k+2\,\lambda))$ term following (2) and (3), since the messages and intrinsic LLR can be normalized accordingly. We also omit the noise modes that appear inside the parentheses to arrive at

$$\rho(b_{\ell}) \approx \left(\max_{i \in B_{\ell}^{0}} s_i \right)^2 - \left(\max_{i \in B_{\ell}^{1}} s_i \right)^2. \tag{16}$$

The key advantage of this last formula is that it does not require knowledge of k or λ, since the latter may alter during the lifetime of the system, and therefore alleviates the requirement for an additional channel estimation subsystem.

The accuracy of the approximations was tested via MC simulations. The simulations were performed using the procedure that was presented in the previous section with the exception that the extrinsic LLR is calculated using the approximate relations (15) and (16) for the sum–product and min-sum decoders, respectively. The approximation results are presented in Fig. 7 and are compared with the ones that have been obtained using the exact LLR expressions. The figure shows that the approximation is highly accurate for $k = 40$, 200 noise modes and the difference is 0.1 dB or less for all modulation orders, data lengths and code rates under consideration. On the other hand, the results for $k = 2$ (not shown) are not accurate and discrepancies up to 0.5 dB were observed. A possible explanation is that the approximation of the χ^2 distributions with gaussians is not accurate enough for a limited number of noise modes.

5. Conclusion

We have presented results on the BEP performance of optically pre-amplified PPM receivers with LDPC error correction codes. The codes are obtained from the latest 5G standard and simulation results demonstrate that a significant real gain can be expected for a range of modulation orders and noise modes. Two popular decoding algorithms have been studied, namely the sum–product and min-sum algorithms, and it was shown that a discrepancy of less 0.2 dB occurs between them for the maximum data length of 8448 bits provided that a suitable code rate is also used. The optimal code rate ranges between 2/3–22/26 for the min-sum decoder and 1/2–22/26 for the sum–product decoder, with higher rates being required at increased modulation orders and noise modes. Finally, we detailed an efficient approximation for the calculation of the external LLR, which both decoders require. The approximation was validated via simulations and it was shown that it is highly accurate (within 0.1 dB) for a high number of noise modes, and therefore of value in practical systems that employ wide optical filters [3].

CRediT authorship contribution statement

Konstantinos Yiannopoulos: Conceptualization, Methodology, Software, Writing – original draft, Writing – review & editing, Visualization. **Nikos C. Sagias:** Conceptualization, Methodology, Software, Writing – original draft, Writing – review & editing, Visualization.

Declaration of competing interest

The authors declare that they have no known competing financial interests or personal relationships that could have appeared to influence the work reported in this paper.

Data availability

No data was used for the research described in the article.

References

[1] D.O. Caplan, B.S. Robinson, R.J. Murphy, M.L. Stevens, Demonstration of 2.5-gslot/s optically-preamplified m-PPM with 4 photons/bit receiver sensitivity, in: Optical Fiber Communication Conference and Exposition and the National Fiber Optic Engineers Conference, Optical Society of America, 2005, p. PDP32, http://dx.doi.org/10.1109/OFC.2005.193210.

[2] D.M. Boroson, J.J. Scozzafava, D.V. Murphy, B.S. Robinson, M.I.T. Lincoln, The lunar laser communications demonstration (LLCD), in: 2009 Third IEEE International Conference on Space Mission Challenges for Information Technology, 2009, pp. 23–28, http://dx.doi.org/10.1109/SMC-IT.2009.57.

[3] M.L. Stevens, D.M. Boroson, A simple delay-line 4-PPM demodulator with near-optimum performance, Opt. Express 20 (5) (2012) 5270–5280, http://dx.doi.org/10.1364/OE.20.005270.

[4] F.I. Khatri, B.S. Robinson, M.D. Semprucci, D.M. Boroson, Lunar laser communication demonstration operations architecture,, Acta Astronaut. 111 (2015) 77–83, http://dx.doi.org/10.1016/j.actaastro.2015.01.023.

[5] H. Nouri, S.M. Sait, M. Uysal, Adaptive modulation for FSO IM/DD systems with multiple transmitters and receivers, IEEE Commun. Lett. 27 (2) (2023) 586–590, http://dx.doi.org/10.1109/LCOMM.2022.3222992.

[6] K. Kiasaleh, Turbo-coded optical PPM communication systems, J. Lightwave Technol. 16 (1) (1998) 18–26, http://dx.doi.org/10.1109/50.654979.

[7] J. Hamkins, Performance of binary turbo-coded 256-ary pulse-position modulation, in: TMO Progress Report 42-13, 1999, pp. 1–15.

[8] S. Dolinar, D. Divsalar, J. Hamkins, F. Pollara, Capacity of pulse-position modulation (PPM) on Gaussian and webb channels, in: TMO Progress Report 42-142, 2000, pp. 1–31.

[9] T. Ohtsuki, Turbo-coded atmospheric optical communication systems, in: 2002 IEEE International Conference on Communications. Conference Proceedings. ICC 2002 (Cat. No.02CH37333), Vol. 5, 2002, pp. 2938–2942, http://dx.doi.org/10.1109/ICC.2002.997378.

[10] B. Moision, J. Hamkins, Coded modulation for the deep-space optical channel: serially concatenated pulse-position modulation, Interplanet. Netw. Prog. Rep. (42–161) (2005) 1–25.

[11] I. Djordjevic, B. Vasic, M. Neifeld, Multilevel coding in free-space optical MIMO transmission with q-ary PPM over the atmospheric turbulence channel, IEEE Photonics Technol. Lett. 18 (14) (2006) 1491–1493, http://dx.doi.org/10.1109/LPT.2006.877576.

[12] S.S. Muhammad, T. Javornik, I. Jelovčan, Z. Ghassemlooy, E. Leitgeb, Comparison of hard-decision and soft-decision channel coded m-ary PPM performance over free space optical links, Eur. Trans. Telecommun. 20 (8) (2009) 746–757, http://dx.doi.org/10.1002/ett.1343, arXiv:https://onlinelibrary.wiley.com/doi/pdf/10.1002/ett.1343.

[13] F. Xu, M.-A. Khalighi, S. Bourennane, Coded PPM and multipulse PPM and iterative detection for free-space optical links, J. Opt. Commun. Netw. 1 (5) (2009) 404–415, http://dx.doi.org/10.1364/JOCN.1.000404.

[14] S. Hu, L. Mi, T. Zhou, W. Chen, 35.88 Attenuation lengths and 3.32 bits/photon underwater optical wireless communication based on photon-counting receiver with 256-PPM, Opt. Express 26 (17) (2018) 21685–21699, http://dx.doi.org/10.1364/OE.26.021685.

[15] S. Haddadi, M. Farhang, M. Derakhtian, Generalized weighted bit-flipping LDPC decoding for asymmetric optical channels, Phys. Commun. 47 (2021) 101369, http://dx.doi.org/10.1016/j.phycom.2021.101369.

[16] T. Richardson, M. Shokrollahi, R. Urbanke, Design of capacity-approaching irregular low-density parity-check codes, IEEE Trans. Inform. Theory 47 (2) (2001) 619–637, http://dx.doi.org/10.1109/18.910578.

[17] H. Pfister, I. Sason, R. Urbanke, Capacity-achieving ensembles for the binary erasure channel with bounded complexity, IEEE Trans. Inform. Theory 51 (7) (2005) 2352–2379, http://dx.doi.org/10.1109/TIT.2005.850079.

[18] D. Divsalar, S. Dolinar, C.R. Jones, K. Andrews, Capacity-approaching protograph codes, IEEE J. Sel. Areas Commun. 27 (6) (2009) 876–888, http://dx.doi.org/10.1109/JSAC.2009.090806.

[19] T. Richardson, S. Kudekar, Design of low-density parity check codes for 5G new radio, IEEE Commun. Mag. 56 (3) (2018) 28–34, http://dx.doi.org/10.1109/MCOM.2018.1700839.

[20] J. Massey, Capacity, cutoff rate, and coding for a direct-detection optical channel, IEEE Trans. Commun. 29 (11) (1981) 1615–1621, http://dx.doi.org/10.1109/TCOM.1981.1094916.

[21] D. Marcuse, Derivation of analytical expressions for the bit-error probability in lightwave systems with optical amplifiers, J. Lightwave Technol. 8 (12) (1990) 1816–1823, http://dx.doi.org/10.1109/50.62876.

[22] P.A. Humblet, M. Azizoglu, On the bit error rate of lightwave systems with optical amplifiers, J. Lightwave Technol. 9 (11) (1991) 1576–1582, http://dx.doi.org/10.1109/50.97649.

[23] N. Alić, G.C. Papen, R.E. Saperstein, L.B. Milstein, Y. Fainman, Signal statistics and maximum likelihood sequence estimation in intensity modulated fiber optic links containing a single optical preamplifier, Opt. Express 13 (12) (2005) 4568–4579, http://dx.doi.org/10.1364/OPEX.13.004568.
[24] T.G. Ulmer, S.R. Henion, F.G. Walther, Power penalty from amplified spontaneous emission in spatial diversity links for fade mitigation, IEEE Photonics Technol. Lett. 21 (3) (2009) 170–172, http://dx.doi.org/10.1109/LPT.2008.2009318.
[25] S. Sahuguede, A. Julien-Vergonjanne, J.-P. Cances, Soft decision LDPC decoding over chi-square based optical channels, J. Lightwave Technol. 27 (16) (2009) 3540–3545, http://dx.doi.org/10.1109/JLT.2009.2022194.
[26] K. Yiannopoulos, N.C. Sagias, A.C. Boucouvalas, Average error probability of an optically pre-amplified pulse-position modulation multichannel receiver under Malaga-M fading, Appl. Sci. 10 (3) (2020) http://dx.doi.org/10.3390/app10031141.
[27] N. Wiberg, Codes and decoding on general graphs, (Ph.D. thesis), Likoping University, 1996.
[28] A. Anastasopoulos, A comparison between the sum-product and the min-sum iterative detection algorithms based on density evolution, in: GLOBECOM'01. IEEE Global Telecommunications Conference, Vol. 2, 2001, pp. 1021–1025, http://dx.doi.org/10.1109/GLOCOM.2001.965572.
[29] J. Zhao, F. Zarkeshvari, A. Banihashemi, On implementation of min-sum algorithm and its modifications for decoding low-density parity-check (LDPC) codes, IEEE Trans. Commun. 53 (4) (2005) 549–554, http://dx.doi.org/10.1109/TCOMM.2004.836563.
[30] M. Jiang, C. Zhao, L. Zhang, E. Xu, Adaptive offset min-sum algorithm for low-density parity check codes, IEEE Commun. Lett. 10 (6) (2006) 483–485, http://dx.doi.org/10.1109/LCOMM.2006.1638623.
[31] V. Savin, Self-corrected min-sum decoding of LDPC codes, in: 2008 IEEE International Symposium on Information Theory, 2008, pp. 146–150, http://dx.doi.org/10.1109/ISIT.2008.4594965.
[32] F. Kschischang, B. Frey, H.-A. Loeliger, Factor graphs and the sum-product algorithm, IEEE Trans. Inform. Theory 47 (2) (2001) 498–519, http://dx.doi.org/10.1109/18.910572.
[33] T. Javornik, I. Jelovčan, S. Sheikh Muhammad, G. Kandus, Simplified soft value extraction for m-PPM-modulated signals in fso systems, AEU - Int. J. Electr. Commun. 63 (7) (2009) 595–599, http://dx.doi.org/10.1016/j.aeue.2008.04.012.
[34] I.S. Gradshteyn, I.M. Ryzhik, Table of Integrals, Series, and Products, seventh ed., Elsevier/Academic Press, Amsterdam, 2007.
[35] M.C. Jeruchim, P. Balaban, K.S. Shanmugan, Simulation of Communication Systems, second ed., Springer, 2000, http://dx.doi.org/10.1007/b117713.
[36] P. Robertson, E. Villebrun, P. Hoeher, A comparison of optimal and sub-optimal MAP decoding algorithms operating in the log domain, in: Proceedings IEEE International Conference on Communications ICC '95, Vol. 2, 1995, pp. 1009–1013, http://dx.doi.org/10.1109/ICC.1995.524253.

Konstantinos Yiannopoulos received the Diploma and Ph.D. in Electrical and Computer Engineering in 2000 and 2004, respectively, from the School of Electrical and Computer Engineering of the National Technical University of Athens, Greece.

Dr. Yiannopoulos is an Assistant Professor at the University of Peloponnese, Greece. He was a member of the research teams of the Photonics Communications Research Laboratory at the National Technical University of Athens, Greece, from 2000 to 2004, and the Computer Networks Laboratory at the University of Patras, Greece, from 2005 to 2010. During this period, he conducted research on physical layer (optical signal processing, ultrafast optical sources, all-optical logic) and network layer (optical packet and burst switching networks) aspects of optical networks. At the present time, he is conducting research that focuses on optical wireless systems and networks.

Dr. Yiannopoulos has more than 70 published papers in international journals and conferences. His research work was granted the "IEEE/LEOS Graduate Student Fellowship Program 2004" award and has received more than 1400 citations.

Nikos C. Sagias was born in Athens, Greece in 1974. He received the B.Sc. degree from the department of Physics (DoP) of the University of Athens (UoA), Greece in 1998. The M.Sc. and Ph.D. degrees in Telecommunication Engineering were received both from the UoA in 2000 and 2005, respectively. Since 2001, he has been involved in various National and European Research & Development projects for the Institute of Space Applications and Remote Sensing of the National Observatory of Athens, Greece. During 2006–2008, was a Postdoc research scholar at the Institute of Informatics and Telecommunications at the National Centre for Scientific Research-"Demokritos", Athens, Greece. During 2008–14 we was an Assistant Professor in the Department of Informatics & Telecommunications at the University of Peloponnese, in Tripolis, Greece, where currently is a Professor. Between 2014–16 he served as the Head of DIT.

Dr. Sagias research interests span the broad area of digital communications, and more specifically include MIMO and cooperative systems, fading channels, satellite communications and optical-wireless communication systems. In his record, he has over fifty (50) papers in prestigious international journals and more than thirty (30) in the proceedings of world recognized conferences. For five (5) years (between 2009–14) he was an Associate Editor of IEEE Transactions on Wireless Communications, while before 2009 he had served as an Editor for AEÜ - International Journal of Electronics and Communications and IETE Technical Review. Additionally, he is serving as a reviewer and TPC member for various IEEE conferences (GLOBECOM, ICC, VTC, etc.). He is a co-recipient of the best paper award in communications in the IEEE Wireless Communications and Networking Conference (WCNC), Istanbul, Turkey, May 2014 and 3rd International Symposium on Communications, Control and Signal Processing (ISCCSP), Malta, March 2008. He is a senior member of the IEEE and IEEE Communications Society as well as the Hellenic Physicists Association.